Supporting information for: Nanoscale Tipping Bucket Effect In A Quantum Dot Transistor-Based Counter

F. Hartmann,[*,†] P. Maier,[†] M. Rebello Sousa Dias,[‡,¶] S. Göpfert,[†] L. K. Castelano,[‡] M. Emmerling,[†] C. Schneider,[†] S. Höfling,[†,§] M. Kamp,[†] Y. V. Pershin,[‖] G. E. Marques,[‡] V. Lopez-Richard,[‡] and L. Worschech[†]

†*Technische Physik and Wilhelm Conrad Röntgen Research Center for Complex Material Systems, Physikalisches Institut, Universität Würzburg, Am Hubland, D-97074 Würzburg, Germany*

‡*Departamento de Física, Universidade Federal de São Carlos, 13565-905, São Carlos, São Paulo, Brazil*

¶*Institute for Research in Electronics and Applied Physics, University of Maryland, College Park, Maryland 20742, USA*

§*SUPA, School of Physics and Astronomy, University of St Andrews, St Andrews, KY16 9SS, United Kingdom*

‖*Department of Physics and Astronomy and USC Nanocenter, University of South Carolina, Columbia, SC 29208, USA*

E-mail: fhartmann@physik.uni-wuerzburg.de

This PDF file includes *i*) description of theoretical model and *ii*) extended data Figs. S1 and S2.

Here we provide some additional information about the analytical model used to simulate

quantum dot-based memory capacitive systems demonstrating the pulse counting capability. First of all, we note that these structures are three-terminal floating gate transistor-like devices in which the gate voltage and side coupled QDs control the current through the quantum constriction (wire). The current through the wire is calculated using the Landauer-Buttiker formalism as

$$I(V_b) = \frac{e}{2\pi} \int_{-\infty}^{\infty} v_n \left[Y(v_n) f_{FD}(E, \mu_L) \right. \\ \left. + Y(-v_n) f_{FD}(E, \mu_R) \right] dk, \tag{1}$$

where v_n is the electron velocity given by $\hbar^{-1}\partial E_n/\partial k$, $f_{FD}(..)$ is the Fermi-Dirac distribution function for electrons, $eV_b = \mu_L - \mu_R$, $\mu_{L(R)}$ are chemical potentials of reservoirs, $Y(..)$ is the step function, and $E_n = E_n^0 + \frac{\hbar^2 k^2}{2m^*}$ with m^* the electron effective mass. Within a single transverse subband approximation, one can find

$$I(V_b) = \frac{e^2}{2\pi\hbar} f_{FD}(E_n^0, \mu) \cdot V_b. \tag{2}$$

In the linear approximation, the quantum dot charge $-en_{dot}$ and the gate voltage V_g shift the transverse subbands energies according to $E_n^0 = \tilde{E}_n^0 + \alpha_0 n_{dot} - \eta_0 V_g$, where α_0 and η_0 are constants and $\tilde{E}_n^0$ are the transverse subbands energies at $n_{dot} = 0$ and $V_g = 0$.

The evolution of n_{dot} is described by a phenomenological rate equation

$$\frac{dn_{dot}}{dt} = - \left[\frac{f(\Delta\epsilon_r)}{\tau_r} + \frac{f(\Delta\epsilon_d)}{\tau_d} \right] \cdot n_{dot} + \frac{f(-\Delta\epsilon_c)}{\tau_c} \tag{3}$$

where τ_i $(i = r, d, c)$ are the time constants for the reset, discharging and charging processes,

$$f(x) = \begin{cases} 1\,, & x < 0 \\ \exp\left(-\frac{x}{kT}\right)\,, & x \geq 0 \end{cases}.$$

and $\Delta\epsilon_i = \epsilon_i + \alpha_i n_{dot} - \eta_i e V_g$ is the energy difference associated with process i. Here, ϵ_i

is the threshold energy for the process i; η_i and α_i are the gate efficiencies and Coulomb interaction constants for this process, and e, the electron charge. According to our experimental observations, the QD charge has no significant effect on the charging and discharging thresholds. Therefore, we stick to the approximation $\alpha_d = \alpha_c = 0$, $\eta_d = \eta_r = 1$. Moreover, the expression for the charging gate efficiency is taken in the form

$$\eta_c = \frac{1}{1 + c_{eff}}, \tag{4}$$

where c_{eff} is the relative quantum capacitance of the channel that depends on n_{dot} as

$$\begin{aligned} c_{eff}\left(n_{dot}, \frac{\mathrm{d}n_{dot}}{\mathrm{d}t}\right) &= Y\left(\frac{\mathrm{d}n_{dot}}{\mathrm{d}t}\right) \cdot G(n_{dot} - n_c) \\ &+ Y\left(-\frac{\mathrm{d}n_{dot}}{\mathrm{d}t}\right) \cdot G(n_{dot} - n_c + \Delta n) \end{aligned} \tag{5}$$

with $G(x) = 1 + 2/\pi \arctan(x/\delta)$. This form of c_{eff} accounts for the memcapacititive bistability observed experimentally. If the capacitance bistability of the channel is sufficiently large and $\tau_r \ll \tau_d$ then the reset term in Eq. (3) provides a fast discharge of the dot (triggered by certain conditions). This form of C_{eff} accounts for the bistability observed in the C-V_g-curve (see Figure 1(c) of the maintext). The bistable capacitance originates from the changing quantum capacitance when charging the QDs. The total gate-channel capacitance can be approximated by the series combination of the geometrical capacitance C_{geo} and the quantum capacitance C_q (see Figure S1 (a)) and follows as [S1–S3]

$$C_{gc} = \left(\frac{1}{C_{geo}} + \frac{1}{C_q}\right)^{-1}. \tag{6}$$

The geometrical capacitance per unit area is determined by the distance, d, between the gate and the channel, $C_{geo} = \epsilon/d$ (ϵ: dielectric constant), and does not depend on V_g. The

quantum capacitance is defined as

$$C_q = \frac{\frac{m^* e^2}{\pi \hbar^2}}{1 + \exp\left(\frac{E_i + \mu_c}{k_b T}\right)} \tag{7}$$

with m^* being the effective mass, e the elementary charge, E_i the energy of the quantized i-th 2-DEG subband, μ_c the electrochemical potential of the channel, and $k_b T$ the thermal energy. For $E_i >> \mu_c$ and $E_i << \mu_c$, the quantum capacitance is negligible or takes the value of the numerator, respectively. In either case, C_q is constant and independent of V_g. Within the range $E_i \approx \mu_c$, μ_c can be approximated as $\mu_c = e\beta V_g$ [S4] and the energy difference $E_i - \mu_c$ follows as $E_i - \mu_c = E_i - e\beta V_g$ leading to a gate voltage-dependent quantum capacitance (see Eq. (7)). Due to the Coulomb interaction of the QDs localized charges, the energy difference $E_i - \mu_c$ is further lifted by charging the QDs and becomes $E_i - \mu_c = E_i + \alpha n - e\beta V_g$. n is the number of electrons on the quantum dots and α can be determined by $\alpha = e/C$, where C is the effective capacitive coupling between the QDs and the channel. Including this energy difference in Eq. (7) leads to the C_q-V_g-dependency

$$C_q = \frac{\frac{m^* e^2}{\pi \hbar^2}}{1 + \exp\left(\frac{E_i + \alpha n - e\beta V_g}{k_b T}\right).} \tag{8}$$

Combining Eqs. (6) and (8) leads to the bistable gate-channel-capacitance as shown in Figures S1 (b) and (c). Charging the quantum dots shifts the quantum capacitance towards larger voltages and as a consequence, the C_{gc}-V_g-curve is bistable. The different gate-channel-capacitances correspond to the two limiting equilibrium charge distributions in the quantum dots.

Let us consider periodic gate voltage sweeps of triangular shape between a minimum and maximum voltages, V_{gs} and V_{gm}, with a fixed voltage increase (decrease) rate ν $(-\nu)$. The period of such sweeps equals to $t_0 = 2(V_{gm} - V_{gs})/\nu$. Using Eq. (3) one can find (taking into account only the discharge term in the right-hand side of Eq. (3)) the remaining number of

localized electrons after N sweeps (without a reset event)

$$n_N^0 = n_0^0 \exp\left(-2N\frac{V_{gm}-\epsilon_d}{\tau_d \nu}\right), \tag{9}$$

where n_0^0 describes the initial charge. To find n_0^0, consider a charging process (given by the last term in the right-hand side of Eq. (3)) starting with $n_{dot}=0$. It follows from a solution of Eq. (3) for the charging process that

$$n_0^0 = \begin{cases} 2\frac{\epsilon_c - V_{gs}}{\tau_c \nu}, & 2\frac{\epsilon_c - V_{gs}}{\tau_c \nu} < n_c \\ n_c, & 2\frac{\epsilon_c - V_{gs}}{\tau_c \nu} \geq n_c \end{cases}, \tag{10}$$

where a saturation value of n_{dot}, n_c, is introduced.

Taking into account the sharp bistability of the capacitance ($\delta \to 0$ in Eq. (5)) and neglecting the reset process in Eq. (3), one can find N^{max} defined as the maximum number of full sweeps without reset before a charging event (that counts as an additional cycle). N^{max} is given by the smallest integer N that fulfills the condition $\exp[-(N+1)t_0/\tau_d(V_{gm} - \epsilon_d)/(V_{gm}-V_{gs})] \leq 1-\Delta n/n_c$. This yields

$$N^{max} = \lfloor -\frac{\tau_d \nu}{2(V_{gm}-\epsilon_d)} \ln(1-\Delta n/n_c) \rfloor,$$

wherer $\lfloor a \rfloor$ represents the floor value of a real number a. The extended data Fig. S2A presents N^{max} as a function of relevant parameters. It's interesting that in the limit $\Delta n/n_c \to 0$ the system evolves within a perpetual single loop as the charging event will be triggered after every discharge.

In the limit $\Delta n/n_c \to 1$ and $T \to 0$ (in this case $f(x) \to Y(x)$), the number of S-cycles before reset can be obtained from the condition that triggers the reset in Eq. (3)

$$\alpha_r n_c \exp\left[-\left(N+\frac{1}{2}\right)\frac{t_0}{\tau_d}\frac{(V_{gm}-\epsilon_d)}{(V_{gm}-V_{gs})}\right] \leq V_{gm}-\epsilon_r \tag{11}$$

yielding

$$N^S = \begin{cases} \lfloor L(V_{gm}) \rfloor, L(V_{gm}) \geq 0 \\ 0, L(V_{gm}) < 0 \end{cases} \tag{12}$$

with $L(V_{gm}) = -\frac{\tau_d \nu}{2(V_{gm}-\epsilon_d)} \ln[(V_{gm}-\epsilon_r)/(\alpha_r n_c)]+1/2$. The total number of gate voltage sweeps in one super-cycle (including all S-cycles and R-cycle) is $N_P = N^S + 1$. The probability to observe an R-cycle can be thus written as

$$P = \frac{1}{1+N^S}. \tag{13}$$

The probability P is plotted in the extended data fig. S2B-E for various values of $\alpha_r n_c$. According our model, for an arbitrary $\Delta n/n_c$, a reset after N^S complete S-cycles will occur if $N^{max} - N^S \geq 0$. In the opposite case of $N^{max} - N^S < 0$, there will be no R-cycles.

The threshold values of V_{gm} corresponding to transitions between super-cycle periods $N^P = N$ and $N^P = N+1$ with $N = 0, 1, 2...$ can be calculated from Eq. (11) keeping the equality sign. Let us denote these thresholds by V_N. Assuming a Gaussian noise distribution of the voltage thresholds, $G(\delta V) = 1/(\sigma\sqrt{2\pi})\exp[-\delta V^2/(2\sigma^2)]$, one can find the probability of super-cycles with $\Delta N = 0, \pm 1, \pm 2, ...$

$$R(\Delta N, V_{gm}) = \int_{V_{j+1+\Delta N}}^{V_{j+\Delta N}} G(\xi - V_{gm}) d\xi, \tag{14}$$

where $V_{gm} \in [V_{j+1}, V_j]$, $j = 0, 1, 2...$, and $V_0 = \infty$. The reproducibility of super-cycles can be characterized by $R(0, V_{gm})$. The probability of an additional or missing sweep in a super-cycle is then given by $R(+1, V_{gm})$ or $R(-1, V_{gm})$, respectively.

The values of model parameters used in our simulations are: $\alpha_r = 0.2$ eV, $\alpha_0 = 0.0003$, $\eta_0 = 0.000035$, $\tau_d = 7.7$ s, $\tau_r = \tau_d/100$, $\tau_c = 1.3$ s, $\epsilon_d = 3.2$ eV, $\epsilon_c = -3.2$ eV, $\epsilon_r = 3.48$ eV, $T = 4.5$K, $\mu = 0.0005$ eV, $\tilde{E}_n^0 = 0$, $\delta = 0.01$, and $\nu = 0.2$ V/s.

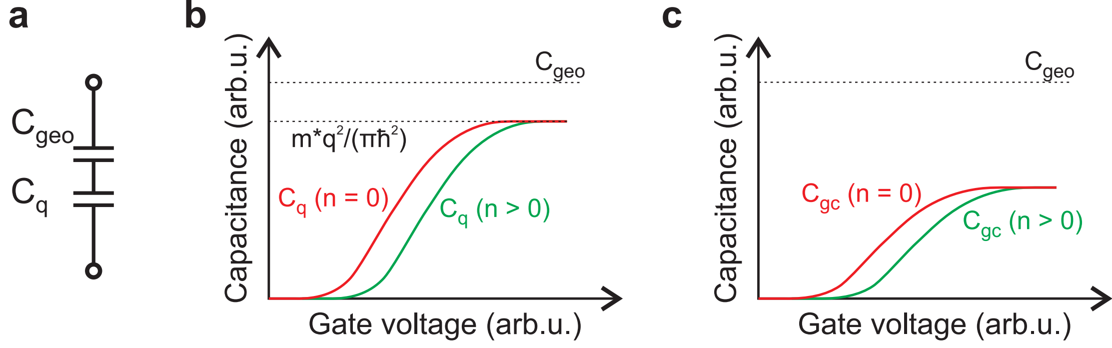

Figure S1: (a) Scheme of the series combination of the geometrical and quantum capacitance, C_{geo} and C_q, respectively, that represent the gate-channel-capacitance C_{gc}. C_{gc} is calculated from the inverse sum of its constituents. (b) Individual values of the capacitances. The geometrical capacitance does not dependent on the gate voltage and is determined by the dielectric constant, ϵ, and the gate-channel distance d. The quantum capacitance is zero when the Fermi energy lies within the energy gap (small gate voltages), increases and takes a constant value, when the Fermi energy lies within the conduction band (see $C_q(n = 0)$). Due to charge localization, the quantum capacitance $C_q(n > 0)$ is shifted towards larger voltages with respect to the initial curve. (c) Gate-channel-capacitance C_{gc} as a function of the gate voltage. The bistability originates from the bistable quantum capacitance (see panel (b)).

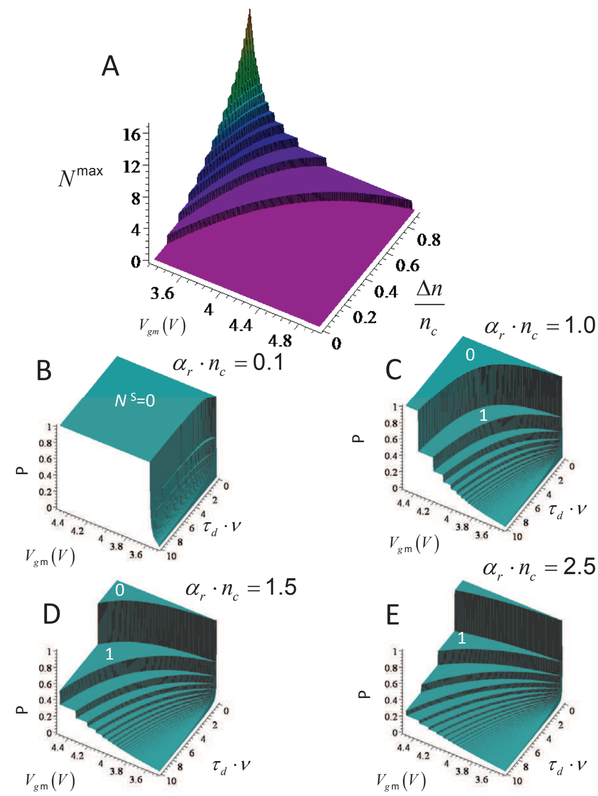

Figure S2: (a) N^{max} as a function of V_{gm} and $\Delta n/n_c$ at $\epsilon_d = 3.2$ eV. (b-e) The probability of reset P as a function of V_{gm} and $\tau_d \nu$ for various values of $\alpha_r n_c$. These plots were obtained at $\epsilon_d = 3.2$ eV.

References

(S1) Luryi, S. *Applied Physics Letters* **1988**, *52*, 501–503.

(S2) Jin, D.; Kim, D.; Kim, T.; del Alamo, J. A. Quantum capacitance in scaled down III-V FETs. 2009 IEEE International Electron Devices Meeting (IEDM). 2009; pp 1–4.

(S3) Hartstein, A.; Albert, N. F. *Phys. Rev. B* **1988**, *38*, 1235–1240.

(S4) Ganeriwala, M. D.; Yadav, C.; Mohapatra, N. R.; Khandelwal, S.; Hu, C.; Chauhan, Y. S. *IEEE Journal of the Electron Devices Society* **2016**, *4*, 396–401.